Inhibitors

DOI: 10.1002/anie.200503003

Fluorescent Inhibitors for IspF, an Enzyme in the Non-Mevalonate Pathway for Isoprenoid Biosynthesis and a Potential Target for Antimalarial Therapy**

Christine M. Crane, Johannes Kaiser, Nicola L. Ramsden, Susan Lauw, Felix Rohdich, Wolfgang Eisenreich, William N. Hunter, Adelbert Bacher,* and François Diederich**

Malaria remains a leading cause of illness and death in endemic areas, infecting 300–500 million and killing 2.5–5 million people annually. As a result of rapidly emerging

[*] N. L. Ramsden, Prof. Dr. W. N. Hunter
Division of Biological Chemistry and Molecular Microbiology
School of Life Sciences
MSI/WTB Complex
University of Dundee
Dow Street, Dundee DD1 5EH (UK)
Fax: (+44) 138-232-2558
E-mail: w.n.hunter@dundee.ac.uk

Dr. J. Kaiser, S. Lauw, Dr. F. Rohdich, Dr. W. Eisenreich, Prof. Dr. A. Bacher
Lehrstuhl für Organische Chemie und Biochemie
Technische Universität München
Lichtenbergstrasse 4, 85748 Garching (Germany)
Fax: (+49) 89-289-13363
E-mail: adelbert.bacher@ch.tum.de

C. M. Crane, Prof. Dr. F. Diederich
Laboratorium für Organische Chemie
ETH Hönggerberg
HCI, 8093 Zürich (Switzerland)
Fax: (+41) 44-632-1109
E-mail: diederich@org.chem.ethz.ch

[**] We gratefully acknowledge financial support for this work from the following agencies: the Hans-Fischer Gesellschaft e.V. (to J.K.), The Wellcome Trust (to W.N.H.), the Biotechnology and Biological Sciences Research Council (UK) (to W.N.H.), and InPharmatica (to W.N.H.). The authors also thank Prof. D. Arigoni and Dr. L. Kemp for help and advice. IspF = 2*C*-Methyl-D-erythritol 2,4-cyclodiphosphate synthase.

Supporting information for this article is available on the WWW under http://www.angewandte.org or from the author.

multiple-drug-resistant strains of the various *Plasmodium* parasites, the search for new therapies with novel modes of action is of urgent necessity.[1] Enzymes in the non-mevalonate pathway, utilized for assembling the C_5 precursors to terpenes, isopentenyl diphosphate (IPP) **1** and dimethylallyl diphosphate (DMAPP) **2**, were recently identified as targets for antimalarial and antimicrobial drugs.[2,3] The non-mevalonate pathway[4] is characterized by the condensation of pyruvate **3** and glyceraldehyde 3-phosphate **4** (Scheme 1) and

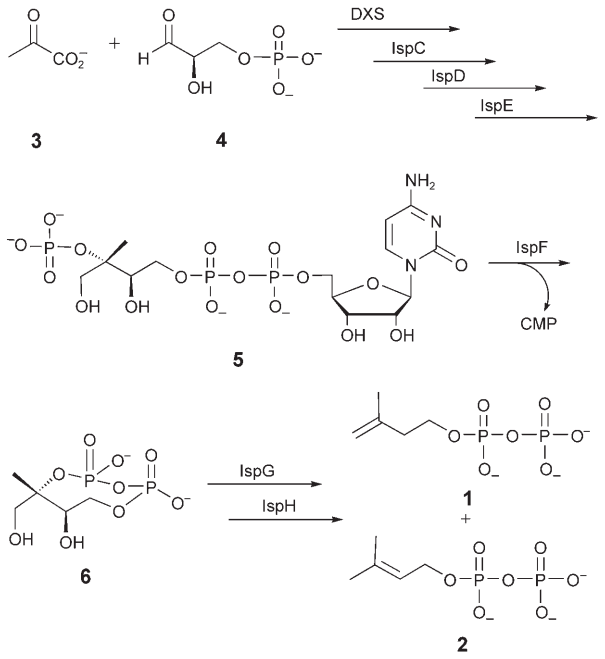

Scheme 1. The non-mevalonate pathway for the biosynthesis of the C_5 precursors to terpenes, IPP **1** and DMAPP **2** (see the Supporting Information). DXS = 1-deoxy-D-xylulose-5-phosphate synthase, CMP = cytidine 5′-monophosphate.[4–8]

is the sole source for **1** and **2** in plastids of higher plants[5a–c] and in many bacteria[4b,5c,6] including some responsible for serious diseases such as *Mycobacterium tuberculosis*[6b] and the protozoan *Plasmodium* parasites (*Apicomplexa*).[3] Since mammals exclusively utilize the mevalonate pathway,[6] the development of small-molecule lead compounds inhibiting the enzymes of the non-mevalonate pathway may be a key step towards new antimalarial drugs.[1b,2,3]

We have chosen the enzyme IspF (2*C*-methyl-D-erythritol 2,4-cyclodiphosphate synthase, *ygbB*) as a target for structure-based lead generation.[7,8] IspF is the fifth enzyme in the non-mevalonate pathway and catalyzes the cyclization of 4-diphosphocytidyl-2*C*-methyl-D-erythritol 2-phosphate (**5**), to the key cyclic diphosphate intermediate, 2*C*-methyl-D-erythritol 2,4-cyclodiphosphate (**6**). Published crystal structures (Protein Data Bank (PDB)[8,9] codes 1GX1 and 1JY8) show IspF to be a C_3-symmetric homotrimer. The topologically equivalent active sites are located at the interfaces of adjacent subunits. The rigid, well-conserved "Pocket III" of one monomer binds the cytidine moiety of **5**, and the larger, more flexible "Pocket II" of an adjacent monomer binds the 2*C*-methyl-D-erythritol moieties of **5** and **6** (for the protein residues lining these pockets, see Figure 1b). The latter pocket also contains a tetrahedrally coordinated Zn^{II} ion.

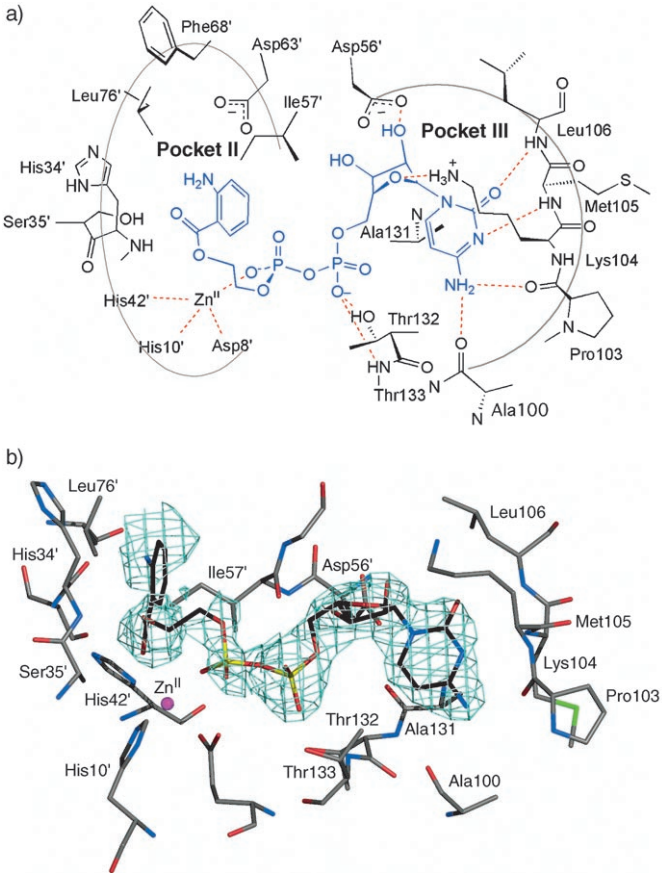

Figure 1. Binding mode of **7** in the ternary complex of IspF with Zn^{II} as determined by X-ray crystallography to 2.3-Å resolution.[17] Ligand binding shown occurs at the interface of subunits A and C (primes designate residues from an adjacent monomer). Five of the six independent active sites of IspF show the depicted binding conformation. a) Schematic representation of the binding mode of **7** (in blue) with potential hydrogen bonds depicted as red dashed lines. b) F_o-F_c omit electron density map surrounded by residues within 4 Å, contoured at the 2σ level. Color code: C gray, O red, N blue, S green, P yellow, Zn^{II} pink ball.

Inhibitors **7**–**9**, occupying both pockets, were designed with the help of the molecular modeling software MOLOC.[10,11] In the absence of known inhibitors, we chose in a first step to maintain the CDP moiety of the natural substrate to occupy Pocket III while connecting the diphosphate by means of an appropriately sized linker to an aromatic residue, for occupation of the hydrophobic cleft of Pocket II, defined by Leu 76′, Phe 61′, and Ile 57′ (Figure 1). Since at a first stage, we were also interested in developing a fluorescence-based enzyme inhibition assay, fluorescent anthranilate (2-aminobenzoate) and dansyl (5,5-dimethylaminonaphthalenesulfamoyl) residues were chosen as aromatic moieties reaching into Pocket II.[12]

The synthesis of target compound **7** is shown in Scheme 2 (for the synthesis of compounds **8** and **9**, see the Supporting Information). Reduction of nitro derivative **10** afforded

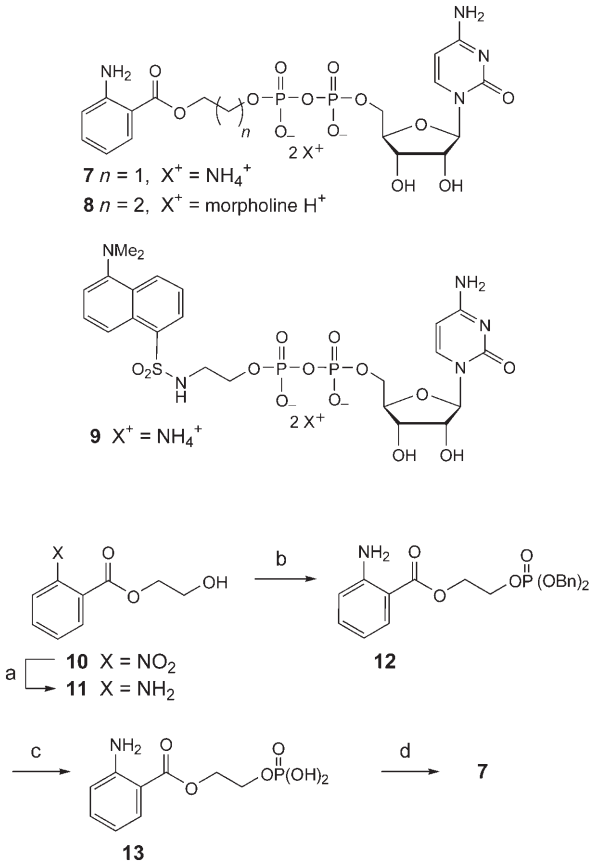

Scheme 2. Synthesis of fluorescent ligand **7**. a) Zn, AcOH, MeOH, 0 °C→20 °C, 5 h, quant.; b) $HOPO(OBn)_2$, DIAD, Ph_3P, THF, 20 °C, 63 %; c) H_2, 10 % Pd/C, CH_2Cl_2/EtOH, 7 h, 20 °C, 98 %; d) Et_3N, cytidine 5′-monophosphomorpholidate 4-morpholine-*N*,*N*′-dicyclohexylcarboxamidine salt, 1*H*-tetrazole, pyridine, 20 °C, 48 h, then DOWEX ion-exchange (NH_4^+), 45 %. THF = tetrahydrofuran, Bn = benzyl, DIAD = diisopropyl azodicarboxylate.

anthranilate **11**, which was phosphorylated using a modified Mitsunobu reaction[13] to furnish phosphotriester **12**. Removal of the benzyl residues by hydrogenation provided the free phosphate **13**. The desired diphosphate was obtained using a modified Moffatt condensation of **13** with cytidine 5′-monophosphomorpholidate 4-morpholine-*N*,*N*′-dicyclohexylcarboxamidine salt, catalyzed by 1*H*-tetrazole.[14] Ion-exchange chromatography (DOWEX 50 WX8 (NH_4^+)) gave the diammonium salt of **7**, which was purified by column chromatography on cellulose and fully characterized (see the Supporting Information).

Fluorescence binding titrations were performed to determine the dissociation constants, K_d, for the complexes of IspF from *Escherichia coli* with ligands **7**–**9**.[15] In the presence of the enzyme, the emission of the fluorescent probes is shifted hypsochromically and increases in intensity (hyperchromism), which is most likely attributed to complexation in an environment of reduced polarity. Affinity data were found to depend substantially on the concentration of Zn^{II} ions present in solution; therefore $Zn(OAc)_2$ was added in a concentration sufficient to ensure saturation of the enzyme. Typical titration curves[15] are depicted in Figure 2. Dissoci-

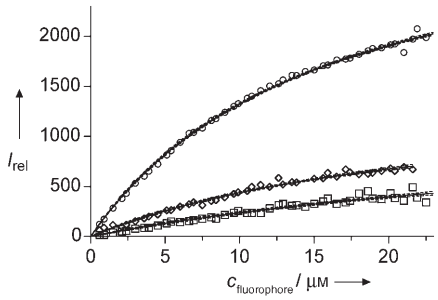

Figure 2. Typical fluorescence titration curves of *E. coli* IspF (6.25 μM) with inhibitors **7** (□), **8** (◇), and **9** (○), measured from 0–24 μM in 0.3-μM aliquots (0.6-μM steps shown for clarity).[15]

ation constants were obtained by nonlinear least-squares approximation and are given in Table 1. All three fluorescent probes show activities in the lower double-digit micromolar

Table 1: Affinities of ligands against *E. coli* IspF measured by fluorescence (**7**–**9**) and ^{13}C NMR assays (**9**, CMP, CDP).

Compound	K_d [μM][a]	IC_{50} [mM][b]
7	36 ± 5	
8	23 ± 2	
9	15 ± 0.3	3.0
CMP		15.0
CDP		7.3

[a] Determined at 25 °C; for details, see ref. [15]. [b] Determined at 37 °C; for details, see ref. [16] and the Supporting Information.

range. In parallel, the IC_{50} values (IC_{50} = concentration of inhibitor at which 50 % of the maximum initial velocity is observed) for **9**, cytidine 5′-diphosphate (CDP), and cytidine 5′-monophosphate (CMP) were determined in enzymatic assays monitored by ^{13}C NMR spectroscopy (see the Supporting Information).[16] These results show inhibitor **9** has a lower IC_{50} value (3.0 mM) than both CDP (7.3 mM) and CMP (15.0 mM), suggesting that binding free enthalpy is gained upon introduction of the aromatic fluorophore on inhibitor **9**. The participation of the fluorescent probes in the binding to the *E. coli* enzyme, as suggested by the fluorescence assays, was subsequently confirmed by X-ray crystal structure analyses of inhibitors **7** and **9** bound to IspF.

The structures of the ternary complexes of **7** (Figure 1) and **9** (see the Supporting Information) with tetrahedrally coordinated Zn^{II} in the active site of *E. coli* IspF were determined to 2.3-Å and to 2.5-Å resolution, respectively.[17] The complex of **7** consists of six subunits (two trimers) in the asymmetric unit, and the complex of **9** consists of one subunit. The crystal structures confirm that the cytidine moieties in both complexes are firmly anchored in Pocket III as predicted. There are four highly conserved hydrogen bonds between the nucleobase, π-stacked against Ala 131, and the backbone from Ala 100 to Leu 106 (see Figure 1a and the Supporting Information).[8,9] The ribose moiety is further held by hydrogen bonds between the ribose C(2′) and C(3′) hydroxyl groups and the carboxylate of Asp 56′. The catalytic Zn^{II} ions in both structures are tetrahedrally coordinated to

the side chains of His10′, His42′, and Asp8′, the fourth coordination site being occupied by the β-phosphate of the inhibitors. The structures confirm our predicted binding mode with the anthranilate and dansyl fluorophores bound in Pocket II.

Two different conformations are observed for the six independent active sites (arbitrarily designated A–F) of IspF in the crystal of the ternary complex with ligand **7** and Zn^{II}. In active sites B–F, the ligand orientation and interactions with the protein are well conserved (see the Supporting Information). The CDP moiety of **7** takes a similar orientation in all six active sites A–F. The imidazole of His34′ in active site A is observed to be in a "closed" (into the active site) conformation, in contrast to the "open" one seen in active sites B–F.[18] Pocket II in structure A shows a higher degree of flexibility, which is mirrored in much larger thermal parameters (see the Supporting Information).

Figure 3 shows the superimposition of the X-ray crystal structures of the ternary complex of IspF-Zn^{II}-**7** (conformers B–F) with the previously reported structure of the quaternary complex of IspF with CMP, **6**, and Zn^{II} (PDB code 1JY8).[8a] In both structures, His34′ adopts the "open" conformation. The anthranilate nicely superimposes with the hydrophobic region of cyclodiphosphate **6**. The loop Leu60′–Phe68′, which shapes the hydrophobic cleft of Pocket II, shows substantial flexibility, approaching the ligands to varying degrees in the two complexes. Interestingly, this flexible loop adopts a nearly identical orientation in the superimposition of the crystal structures of the ternary complex IspF-Zn^{II}-**7** and the quaternary complex IspF-Zn^{II}-Mn^{II}-CDP (PDB code 1GX1).[8b] On the other hand, His34′ assumes the "closed" conformation in the latter complex to interact with the β-phosphate of CDP (see the Supporting Information).

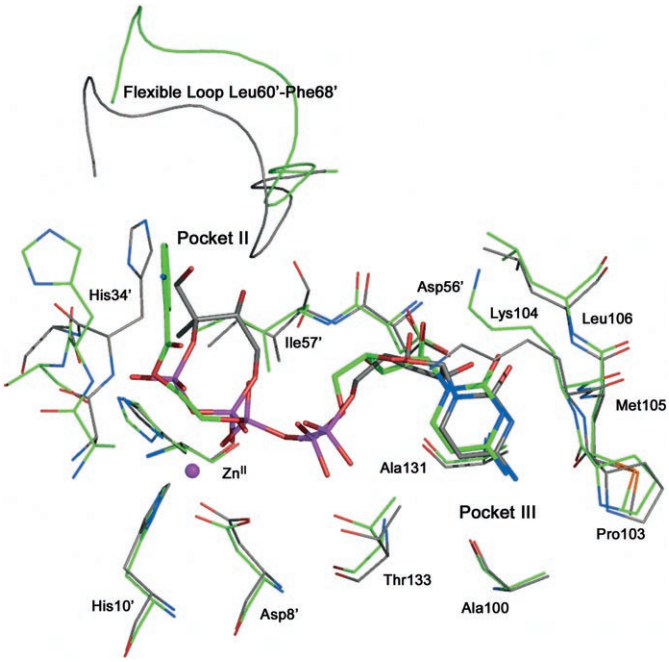

Figure 3. Superimposition of the X-ray crystal structures of the ternary complex of IspF-Zn^{II}-**7** (conformers B–F; C atoms: light-green) with the previously reported structure of the quaternary complex of IspF with CMP, 2C-methyl-D-erythritol 2,4-cyclodiphosphate (**6**), and Zn^{II} (PDB code 1JY8;[8a] C atoms: gray). Color code: O red, N blue, S red-orange, P purple, Zn^{II} ion: purple ball.[17]

The crystals of the ternary complex of IspF bound to **9** and Zn^{II} contain a single monomer in the asymmetric unit. Interactions in the cytidine pocket mirror those seen for the complex with **7** (see the Supporting Information). His34′ adopts an "open" conformation. A superimposition of the X-ray crystal structures of the enzyme bound to **7** and **9** (see the Supporting Information) provides additional evidence for the large conformational flexibility of the hydrophobic cleft of Pocket II. Compared to the complex of **7**, the lipophilic residues Ile56′, Phe61′, Phe68′, and Leu76′ interacting with **9** have undergone a considerable reorientation to accommodate the larger dansyl residue and engage in hydrophobic enzyme–ligand contacts. The F_o-F_c omit electron density map of bound **9** shows only weak electron density about the dansyl ring and elevated thermal parameters suggest a large degree of flexibility (see the Supporting Information).

In conclusion, we have reported the synthesis, biological evaluation, and co-crystal structures of the first designed inhibitors of IspF. By introducing fluorescent probes in inhibitors **7**–**9**, we could determine their affinity towards IspF by fluorescence binding titrations. Efforts to validate the utility of the fluorescent inhibitors as standards in rapid and economic affinity assays are ongoing. The predicted binding modes of **7** and **9** were largely confirmed by X-ray crystal structure analysis. Although the hydrophobic region in Pocket II apparently is very flexible, its occupation by aromatic rings leads to a measurable gain in binding free enthalpy. The results provide fruitful guidance for the future development of new inhibitors of the non-mevalonate pathway, by structure-based design, with the promise to ultimately generate new classes of antimalarials and other antimicrobials.

Received: August 23, 2005
Published online: January 3, 2005

Keywords: fluorescence · inhibitors · IspF · non-mevalonate pathway · protein crystal structure analysis

[1] a) U. Weiss (Ed.), "Malaria", in *Nature* **2002**, *415*, 669–715; b) L. Schofield, M. C. Hewitt, K. Evans, M.-A. Siomos, P. H. Seeberger, *Nature* **2002**, *418*, 785–789; c) J. K. Baird, *N. Engl. J. Med.* **2005**, *352*, 1565–1577.

[2] Fosmidomycin (OHC-N(OH)-$(CH_2)_3$-PO_3H_2) is a potent inhibitor of 1-deoxy-D-xylulose-5-phosphate reductoisomerase (IspC) in the non-mevalonate pathway. For some selected publications, see: a) J. Wiesner, R. Ortmann, H. Jomaa, M. Schlitzer, *Angew. Chem.* **2003**, *115*, 5432–5451; *Angew. Chem. Int. Ed.* **2003**, *42*, 5274–5293; b) T. Kuzuyama, T. Shimizu, S. Takahashi, H. Seto, *Tetrahedron Lett.* **1998**, *39*, 7913–7916; c) M. A. Missinou, S. Borrmann, A. Schindler, S. Issifou, A. A. Adegnika, P.-B. Matsiegui, R. Binder, B. Lell, J. Wiesner, T. Baranek, H. Jomaa, P. G. Kremsner, *Lancet* **2002**, *360*, 1941–1942; d) B. Lell, R. Ruangweerayut, J. Wiesner, M. A. Missinou, A. Schindler, T. Baranek, M. Hintz, D. Hutchinson, H. Jomaa,

P. G. Kremsner, *Antimicrob. Agents Chemother.* **2003**, *47*, 735–738.

[3] H. Jomaa, J. Wiesner, S. Sanderbrand, B. Altincicek, C. Weidemeyer, M. Hintz, I. Türbachova, M. Eberl, J. Zeidler, H. K. Lichtenthaler, D. Soldati, E. Beck, *Science* **1999**, *285*, 1573–1576.

[4] a) W. Eisenreich, M. Schwarz, A. Cartayrade, D. Arigoni, M. H. Zenk, A. Bacher, *Chem. Biol.* **1998**, *5*, R221–R233; b) M. Rohmer, M. Knani, P. Simonin, B. Sutter, H. Sahm, *Biochem. J.* **1993**, *295*, 517–524.

[5] a) M. K. Schwarz, PhD Dissertation, ETH Zürich, No. 10951, **1994**; b) W. Eisenreich, B. Menhard, P. J. Hylands, M. H. Zenk, A. Bacher, *Proc. Natl. Acad. Sci. USA* **1996**, *93*, 6431–6436; c) S. T. J. Broers, PhD Dissertation, ETH Zürich, No. 10978, **1994**.

[6] a) F. Rohdich, S. Hecht, A. Bacher, W. Eisenreich, *Pure Appl. Chem.* **2003**, *75*, 2–3, 393–405; b) Y. Boucher, W. F. Doolittle, *Mol. Microbiol.* **2000**, *37*, 703–716; c) F. Rohdich, J. Wungsintaweekul, M. Fellermeier, S. Sanger, S. Herz, K. Kis, W. Eisenreich, A. Bacher, M. H. Zenk, *Proc. Natl. Acad. Sci. USA* **1999**, *96*, 11758–11763.

[7] For selected publications, see: a) F. Rohdich, W. Eisenreich, J. Wungsintaweekul, S. Hecht, C. A. Schuhr, A. Bacher, *Eur. J. Biochem.* **2001**, *268*, 3190–3197; b) S. B. Richard, J.-L. Ferrer, M. E. Bowman, A. M. Lillo, C. N. Tetzlaff, D. E. Cane, J. P. Noel, *J. Biol. Chem.* **2002**, *277*, 8667–8672; c) T. L. Campbell, E. D. Brown, *J. Bacteriol.* **2002**, *184*, 5609–5618.

[8] a) S. Steinbacher, J. Kaiser, J. Wungsintaweekul, S. Hecht, W. Eisenreich, S. Gerhardt, A. Bacher, F. Rohdich, *J. Mol. Biol.* **2002**, *316*, 79–88; b) L. E. Kemp, C. S. Bond, W. N. Hunter, *Proc. Natl. Acad. Sci. USA* **2002**, *99*, 6591–6596.

[9] Published crystal structures of IspF: a) H. Kishida, T. Wada, S. Unzai, T. Kuzuyama, M. Takagi, T. Terada, M. Shirouzu, S. Yokoyama, J. R. H. Tame, S.-Y. Park, *Acta Crystallogr. D* **2003**, *59*, 23–31; b) S. Ni, H. Robinson, G. C. Marsing, D. E. Bussiere, M. A. Kennedy, *Acta Crystallogr. D* **2004**, *60*, 1949–1957; c) C. Lehmann, K. Lim, J. Toedt, W. Krajewski, A. Howard, E. Eisenstein, O. Herzberg, *Proteins: Struct. Funct. Bioinf.* **2002**, *49*, 135–138; d) L. E. Kemp, M. S. Alphey, C. S. Bond, M. A. J. Ferguson, S. Hecht, A. Bacher, W. Eisenreich, F. Rohdich, W. N. Hunter, *Acta Crystallogr. D* **2005**, *61*, 45–52; e) T. Sgraja, L. E. Kemp, N. L. Ramsden, W. N. Hunter, *Acta Crystallogr. F* **2005**, *61*, 625–629.

[10] a) P. R. Gerber, K. Müller, *J. Comput.-Aided Mol. Des.* **1995**, *9*, 251–268; b) Gerber Molecular Design (http://www.moloc.ch).

[11] For structure-based design of inhibitors of plasmepsin II, another potential target in antimalarial therapy, see: D. Carcache, S. Hörtner, A. Bertogg, C. Bonkert, D. Bur, H. P. Märki, A. Dorn, F. Diederich, *ChemBioChem* **2002**, *3*, 1137–1141.

[12] a) Y.-H. Li, L.-M. Chan, L. Tyler, R. T. Moody, C. M. Himel, D. M. Hercules, *J. Am. Chem. Soc.* **1975**, *97*, 3118–3126; b) F. Diederich, K. Dick, D. Griebel, *Chem. Ber.* **1985**, *118*, 3588–3619.

[13] M. Saady, L. Lebeau, C. Mioskowski, *Tetrahedron Lett.* **1995**, *36*, 2239–2242.

[14] V. Wittmann, C.-H. Wong, *J. Org. Chem.* **1997**, *62*, 2144–2147.

[15] a) The fluorescent inhibitors **7–9** were titrated into a solution (2 mL) of IspF (17 kDa per subunit) from *E. coli* (6.25 μM) in 50 mM Tris hydrochloride, pH 8.2, containing 10 mM $MgSO_4$ and 2 mM $ZnO(Ac)_2$ in a total volume of 3 mL at 20 °C (Tris = tris(hydroxymethyl)aminomethane). Spectral data were recorded at $\lambda_{exc} = 320$ nm, $\lambda_{em} = 423$ nm for compounds **7** and **8**, and $\lambda_{exc} = 366$ nm, $\lambda_{em} = 532$ nm for **9**, using a Hitachi F-2000 fluorescence spectrophotometer (1-cm quartz cuvette, 3-mL volume). K_d values were derived using Equation (1):

$$I_{rel} = (I_{max} F_o)(K_d + F_o)^{-1} \quad (1),$$

where I_{rel} is the relative fluorescence intensity at the recorded emission wavelength, I_{max} the maximal fluorescence enhancement of bound inhibitor at saturation, and F_o is the concentration of the fluorophore. Background emissions of **7–9** (from 0–24 μM) as well as of IspF in 50 mM Tris hydrochloride, pH 8.2, containing 10 mM $MgSO_4$ and 2 mM $Zn(OAc)_2$, were subtracted to obtain the saturation curves shown in Figure 2. The relative fluorescence enhancements $(I_{max}-I)/I$, where I is the maximum fluorescence of the unbound inhibitor, were 20% (**7**), 30% (**8**), and 80% (**9**). Binding data were analyzed by nonlinear least-squares approximation (GraphPad Prism 4 Software, San Diego, CA, 2005). Uncertainties given are standard deviations, with R^2 for all fits ≥ 0.96); b) R. S. Sarfati, V. K. Kansal, H. Munier, P. Glaser, A.-M. Gilles, E. Labruyère, M. Mock, A. Danchin, O. Bârzu, *J. Biol. Chem.* **1990**, *265*, 18902–18906; c) W. O. McClure, G. M. Edelman, *Biochemistry* **1967**, *6*, 559–566.

[16] The IC_{50} values for CMP, CDP, and **9** were determined in enzymatic reactions catalyzed by the *E. coli* IspF enzyme using [1,3,4-$^{13}C_3$]-**5** (1 mM) as substrate. Product formation was monitored by ^{13}C NMR spectroscopy (see the Supporting Information).

[17] a) Crystals of *E. coli* IspF complexed with ligands **7** or **9** were grown by the vapor-diffusion method.[8b] The reservoir solution was 0.1 M ammonium sulfate and 0.1 M sodium acetate, pH 5, and 10% and 8% monomethylether polyethylene glycol 200 for compounds **7** and **9**, respectively. The hanging drops consisted of 1 μL of reservoir and 3 μL of a solution of IspF (5.5 mg mL^{-1}) in 50 mM Tris (tris(hydroxymethyl)aminomethane) hydrochloride, pH 7.7, containing 50 mM NaCl and 2 mM ligand. Crystals of the complex with **7** are monoclinic plates in the space group $P2_1$ with unit cell dimensions $a = 54.03$, $b = 115.27$, $c = 87.61$ Å, $\beta = 90.18°$. Crystals of the complex with **9** are cubic blocks in the space group $I2_13$ with $a = 145.1$ Å. Data were measured on beamline ID29 at the European Synchrotron Radiation Facility (Grenoble, France) and processed with MOSFLM (A. G. W. Leslie, H. R. Powell, G. Winter, O. Svensson, D. Spruce, S. McSweeney, D. Love, S. Kinder, E. Duke, C. Nave, *Acta Crystallogr. D* **2002**, *58*, 1924–1928). The dataset for the complex of **7** is 99.5% complete to 2.3-Å resolution with an R_{sym} value of 9.7%, 27.1% in the highest resolution bin. The dataset for the complex of **9** is 99% complete to 2.5-Å resolution with an R_{sym} value of 8%, 68.5% in the highest resolution bin. The starting model for both analyses was the structure of *E. coli* IspF in complex with CDP (PDB code 1GX1). Molecular replacement methods (Collaborative Computational Project Number 4, *Acta Crystallogr. D* **1994**, *50*, 760–763; J. Navaza, *Acta Crystallogr. Sect. D* **2001**, *57*, 1367–1372) were used to generate the starting models for refinement, which consisted of six subunits (two trimers) for the complex with **7** and a single subunit for the complex with **9**. The structures were refined using a combination of O (T. A. Jones, J. Y. Zou, S. W. Cowan, M. Kjeldgaard, *Acta Crystallogr. A* **1991**, *47*, 110–119) and refmac5 (G. N. Murshudov, A. A. Vagin, E. J. Dodson, *Acta Crystallogr. D* **1997**, *53*, 240–255) to an R factor of 24.3% and R-free of 27.9% for the complex with **7**; an R factor of 21.5% and R-free of 25.9% for the complex of **9**. The model for the complex of **7** includes 233 water molecules, six Zn^{II} ions, one in each active site and two molecules of geranyldiphosphate (GPP).[9d] A total of 92.1% of the residues are in the most favored regions of the Ramachandran plot with none in disallowed regions. The model for the complex of **9** includes 56 water molecules, a Zn^{II} ion, and one geranyldiphosphate; 90.8% of the residues are in the most favored regions of the Ramachandran plot with none in disallowed regions. Further details are included in the Protein Data Bank depositions PDB codes: 2AMT and 2AO4; b) It should be noted that a screen of crystallization conditions were

explored to generate useful crystals, and the best conditions did not have Mg^{II} present for either ligands **7** and **9**. Crystals with other ligands in the presence and absence of Mg^{II} or Mn^{II} have been grown in the past; structural differences that can be attributed to the presence/absence of the divalent cations could not be observed (unpublished data).

[18] a) The imidazole ring of His34′ in active sites B–F is observed to varying degrees to be in an "open" (away from the active site) conformation. Distances from the anthranilate NH_2 to the imidazole ring range from 3.8 to 4.5 Å, thereby precluding the presence of any strong interaction. The "open" and "closed" conformations of His34′ have been observed in some of the previously reported crystal structures of IspF.[8,9] b) Deviation in active site A cannot be attributed to crystal-packing effects.

